Dependence of the vibrational spectra of amorphous silicon on the defect concentration and ring distribution

1999 J. Phys.: Condens. Matter 11 9647

(http://iopscience.iop.org/0953-8984/11/48/321)

J. Phys.: Condens. Matter **11** (1999) 9647–9658. Printed in the UK PII: S0953-8984(99)07151-9

Dependence of the vibrational spectra of amorphous silicon on the defect concentration and ring distribution

N Zotov†¶, M Marinov‡, N Mousseau§ and G Barkema‖

† Bayerisches Geoinstitut, Universität Bayreuth, D-95440 Bayreuth, Germany
‡ Central Laboratory of Mineralogy and Crystallography, Sofia 1000, Bulgaria
§ Department of Physics and Astronomy, Ohio University, Athens, OH 45701, USA
‖ Theoretical Physics, Utrecht University, Princetonplein 5, 3584 CC Utrecht, The Netherlands

E-mail: nikolay.zotov@uni-bayreuth.de

Received 23 August 1999

Abstract. The Raman spectra of nine 216-atom models of amorphous silicon (a-Si) are calculated using the bond polarizability approximation of Raman scattering. These a-Si models, generated by the activation relaxation technique, have different concentrations of coordination defects, ring statistics and local strain distributions, which cause changes in the vibrational density of states and the Raman scattering. Analysis of the vibrational modes indicates that an increase in the number of coordination defects leads to an increase in the high-frequency localization and to mixing of the TA modes with other high-frequency modes. Calculation of partial Raman spectra indicates that five-coordinated Si atoms enhance the high-frequency part of the LO Raman peak at about 400 cm^{-1} and lead to characteristic band at about 600 cm^{-1} on the high-frequency side of the TO Raman peak. For their part, the three-coordinated Si atoms contribute to the low-frequency part of the LO peak. A weak correlation between the number of four-membered rings and the intensity of the LO Raman peak is also established although there is no correlation between the number of three- and four-membered rings and the total strain energy.

1. Introduction

The theoretical investigation of the vibrational properties of amorphous silicon (a-Si) has been an active area of research over the past 25 years. Most of the recent studies represent qualitative comparisons of the vibrational density of states (VDOS) of structural models constructed by different methods. Only a few quantitative relationships between the structure and the vibrational properties, such as the linear correlation between the linewidth of the transverse-optic (TO) Raman peak (Γ_{TO}) and the degree of tetrahedral angle disorder [1] or the hydrogen content [2], exist.

Despite the great influence of coordination defects on the width of the band gap in a-Si [3], there are only a few qualitative studies of their effect on the vibrational spectra which are restricted only to the vibrational density of states and the participation ratio of the vibrational modes [4–7]. Studies of the effects of the network topology on the vibrational spectra, with the exception of [8] and [9], where the effect of voids on the VDOS was studied, are practically nonexistent.

It is well established that an increase of the short-range disorder, in other words, the local strain in the network, leads to an increase in the linewidth of the TO Raman peak

¶ Corresponding author.

and to a decrease of its frequency [1, 10, 11]. The experimental separation and investigation of the effects of coordination defects and ring distribution by Raman spectroscopy is not straightforward, however. a-Si can only be prepared in thin films and other factors, such as method of preparation, substrate temperature, deposition rate, thermal annealing and residual H concentration, also affect the local strain distribution and network topology and thus lead to changes in the Raman spectra.

In the present work we have calculated the Raman spectra, the VDOS and the character of the vibrational modes of nine structural models of a-Si with different defect concentrations and ring distributions constructed by the recently proposed activation–relaxation technique [12, 13]. A model for the first-order Raman scattering in the bond polarizabilty approximation [14] is used for the calculations of the spectra. The effect of small (three- and four-membered) rings and coordination defects (three- and five-coordinated Si atoms) on the Raman spectra of the models is studied in detail by analysing the corresponding partial Raman spectra and characteristic spectral ranges for identifying such structural features in experimental Raman spectra are determined.

2. Calculation procedures

The models are constructed following the activation–relaxation technique procedure described in [13]. We start with a 216-atom randomly packed cell with periodic boundary conditions and box edge $L \sim 16.6$ Å. Previous studies on VDOS of a-Si [4, 7] using models of different size have shown that except at very low and very high frequencies, there is not much information in the VDOS of larger a-Si models which is not already present in the 216-atom models. The initial density of the models is slightly below that of crystalline silicon (c-Si). Each model is then optimized through a series of activation–relaxation steps: (1) a given configuration is brought from a local minimum to a nearby saddle-point (activation) then (2) relaxed using a local energy-minimization procedure including volume optimization. The final densities are between 4 and 6% lower than that of c-Si, compared with about 2–3% lower densities for high-quality chemical vapour-deposited (CVD) a-Si. We use a modified Stillinger–Weber (SW) potential with an enhanced angular force [15, 16], which leads to amorphous configurations with structural properties in excellent agreement with experiment [12, 16].

Although the modified SW potential gives correct static structures, it is not designed to reproduce the direct interaction between silicon atoms (see for example [6] and [15]) and thus the dynamical properties should be studied with other types of interaction. Such a type of mixed approach has been widely used in vibrational calculations on a-Si (see for example [1] and [4]).

In the present study we use a Kirkwood-type harmonic potential [17], which is especially suited for vibrational studies of covalently bonded materials. We first perform structural relaxation of all models using the Kirkwood potential. The equilibrium Si–Si bond length was set equal to the experimentally observed Si–Si distance of 2.36 Å [18] and the equilibrium Si–Si–Si bond angle to the ideal tetrahedral value $\Theta_0 = 109.47^\circ$. The minimization of the strain energy is achieved by an iterative process in which each atom is displaced one at a time in the direction of the force without allowing bond breaking or reconstruction. This process is repeated until convergence is achieved (typically within ten cycles). The average shift of the atoms in the relaxed models varies from about 0.056 Å for model 8, which has the lowest total strain energy, as given by the Kirkwood potential, to 0.096 Å for model 3, which has the highest total strain energy and the largest number of defects.

The VDOS is calculated by direct diagonalization of the dynamical matrix. The values of the stretching and bending force constants used for energy relaxation and VDOS

calculations are 125 and 5 N m^{-1}, respectively; they were adjusted previously [14] to reproduce approximately the position of the main vibrational bands of a-Si.

To characterize the phase relationship between vibrations of neighbouring atoms we calculate for each eigenmode p the phase quotient $\mathrm{PQ}(\omega_p)$, using the formula originally introduced by Bell and Hibbins-Butler [19]

$$\mathrm{PQ}(\omega_p) = \sum_m \boldsymbol{u}_p^\alpha \cdot \boldsymbol{u}_p^\beta \Big/ \sum_m |\boldsymbol{u}_p^\alpha \cdot \boldsymbol{u}_p^\beta| \tag{1}$$

where atoms α and β form the bond m, $\boldsymbol{u}_p^\alpha$ is the displacement vector of atom α when it vibrates in mode p and the summation is over all nearest-neighbour bonds in the model. Since the acoustic and optic modes induce respectively in-phase and anti-phase displacements between neighbouring atoms, the phase quotient shifts from +1 to -1 as the atomic vibrations change from mostly acoustic to mostly optic in character. Information about the degree of mode localization can be obtained either from the participation ratio (see [4], [7] and [14]) or from the correlation length $L_c(\omega_p)$ of a single mode p defined by

$$L_c^2(\omega_p) = \sum_\alpha |\boldsymbol{r}^\alpha - \boldsymbol{r}_p|^2 |\boldsymbol{u}_p^\alpha|^2 \Big/ \sum_\alpha |\boldsymbol{u}_p^\alpha|^2 \tag{2}$$

where $\boldsymbol{r}^\alpha$ is the radius vector of atom α and $\boldsymbol{r}_p$ is the centre of gravity of mode p defined by

$$\boldsymbol{r}_p = \sum_\alpha \boldsymbol{r}^\alpha |\boldsymbol{u}_p^\alpha|^2 \Big/ \sum_\alpha |\boldsymbol{u}_p^\alpha|^2. \tag{3}$$

$L_c(\omega_p)$ represents a length beyond which the amplitude of the atomic vibrations decreases significantly. $L_c(\omega_p)$ should therefore be small for highly localized modes and about $L/2$ for highly delocalized modes, where L is the box edge.

For the calculation of the first-order Raman spectra of the structural models we use the mean bond polarizability approximation [20, 21] in which the induced polarizability tensor α of mode p is written in the form

$$\alpha_{ij}^p = \bar{A}' \sum_m \Delta u_m^p \hat{r}_{ab} \delta_{ij} + \bar{\gamma}' \sum_m \Delta u_m^p \hat{r}_{ab} (\hat{r}_{ab}\hat{r}_{ab} - 1)_{ij}$$
$$+ \bar{\gamma} \sum_m \frac{1}{R_{ab}} (\Delta u_m^p \hat{r}_{ab} + \hat{r}_{ab} \Delta u_m^p - 2\Delta u_m^p \hat{r}_{ab}\hat{r}_{ab}\hat{r}_{ab})_{ij} \tag{4}$$

where γ is the mean perpendicular bond polarizability, A is the mean parallel bond polarizability, γ' and A' are the derivatives of γ and A with respect to R_{ab}, R_{ab} is the length of bond m between atoms a and b, $\hat{r}_{ab}$ is a unit vector along the mth bond, $\Delta u_m^p = u_p^a - u_p^b$ and the summation is over all nearest-neighbour Si–Si bonds. Detailed description of the calculation of the polarized (VV and VH) intensities, using the polarizability tensor α is given elsewhere [22]. In the present calculations we assume that the perpendicular bond polarizability does not depend on R, e.g. that $\gamma' \equiv 0.0$. In this case the depolarization ratio $\rho = I_{VH}/I_{VV}$ depends only on the ratio γ/A' rather than on their absolute values, which are adjusted to give the experimentally observed average depolarization ratio of about 0.5 [11, 23]. Each Raman line is additionally broadened by 15 cm^{-1} in order to account for the finite size of the models and additional disorder not present in the generated computer models. The additional line broadening was selected to reproduce approximately the experimentally determined linewidth of the TO Raman peak (see below).

The partial Raman spectra of atom clusters in a given model are calculated using the atomic displacements obtained by projecting the contribution of these atoms and their nearest neighbours out of the dynamical matrix. In particular, the partial Raman spectra of an n-membered ring are calculated taking into account the contribution from the n bonds forming the ring and then averaging the spectra for all rings of equal size.

3. Results

The total strain energy (E), as given by the Kirkwood potential, the number of three-coordinated (D_3) and five-coordinated (D_5) Si atoms, the number of three-membered (R_3), four-membered (R_4), five-membered (R_5) and six-membered (R_6) rings, as well as the average angular ($\langle\Delta\Theta\rangle$) and radial ($\langle\Delta r\rangle$) tetrahedral distortions of the relaxed models are given in table 1.

Table 1. Structural characteristics of the investigated a-Si models: total energy (E); average coordination (CN); number of three-fold coordinated (D_3) and five-fold coordinated (D_5) Si atoms; number of three-membered (R_3), four-membered (R_4), five-membered (R_5) and six-membered (R_6) rings; average angular ($\langle\Delta\Theta\rangle$) and radial ($\langle\Delta r\rangle$) tetrahedral distortions.

Model	E (eV) $\times 10^2$	CN[a]	D_3	D_5	R_3	R_4	R_5	R_6	$\langle\Delta\Theta\rangle$ (°)	$\langle\Delta r\rangle$ (Å)
1	5.1655	4.01 ± 0.14	1	3	0	8	96	183	8.97	0.034
2	5.5811	4.01 ± 0.24	5	7	0	2	99	186	8.76	0.035
3	6.4086	4.05 ± 0.27	3	13	1	14	98	189	8.75	0.036
4	5.1906	4.00 ± 0.24	6	6	0	5	94	176	8.75	0.036
5	5.1490	3.99 ± 0.19	3	3	0	2	96	185	8.94	0.036
6	4.9842	4.02 ± 0.19	2	6	1	6	91	194	8.24	0.031
7	4.3890	3.98 ± 0.13	4	0	0	0	88	184	8.43	0.031
8	4.2545	4.00 ± 0.17	3	3	0	1	87	211	7.95	0.031
9	5.1147	4.01 ± 0.19	3	5	0	3	90	193	8.45	0.032

[a] Calculated assuming a bond between two Si atoms, if their separation is below 3 Å. The errors in the average CN are calculated from the corresponding coordination number distributions.

Similarly to tight-binding [24], *ab initio* [25] and classical [26] molecular dynamics simulations of a-Si, the ART technique also generates three- and five-coordinated defects, but the Si–Si first-nearest-neighbour coordination number for all models is close to 4.0 (see table 1) in agreement with experimentally obtained values of about 3.9 ± 0.2 in annealed a-Si thin films (see for example [18]). Within the uncertainties, experiments tend to support a fourfold coordinated continuous random network, although a coordination as low as 3.79 in as-implanted a-Si membranes prepared by ion bombardment was recently reported [27]. The origin of this discrepancy is still open at the moment. There is a weak correlation between the total strain energy and the total number of defects, as well as between the total energy and the average tetrahedral distortion $\langle\Delta\Theta\rangle$, but there is no correlation between the total strain energy and the number of three- and four-membered rings in the investigated models.

The vibrational density of states (VDOS) is generally independent of the details of the models (figure 1) and compares well with the experimental neutron scattering measurements [28, 29]. In particular, the intensity ratio of the TA to the TO peak in VDOS of about 0.83 is very close to the value of 0.88 obtained from neutron inelastic scattering measurements [29]. The calculated VDOSs are in good agreement also with previous VDOS calculations for a-Si models constructed by different methods and using various potentials [4, 7–9, 14, 24, 30]. This indicates that the trends observed in the calculations are real and not strongly model dependent. The major difference between the VDOS spectra of the investigated models is in the height of the TO peak. There is a general trend for decreasing the height of this peak with increasing defect concentration. However, for models with equal numbers of defects the decrease of the TO VDOS peak is larger for models with larger total strain energy. These results confirm the conclusions from previous studies that the height of the TO peak is related to the concentration of defects [2, 5] and the degree of distortion of the Si tetrahedra [5, 6]. We observe also slight increase of the linewidth of the LA VDOS peak with increasing number of coordination defects and total strain energy.

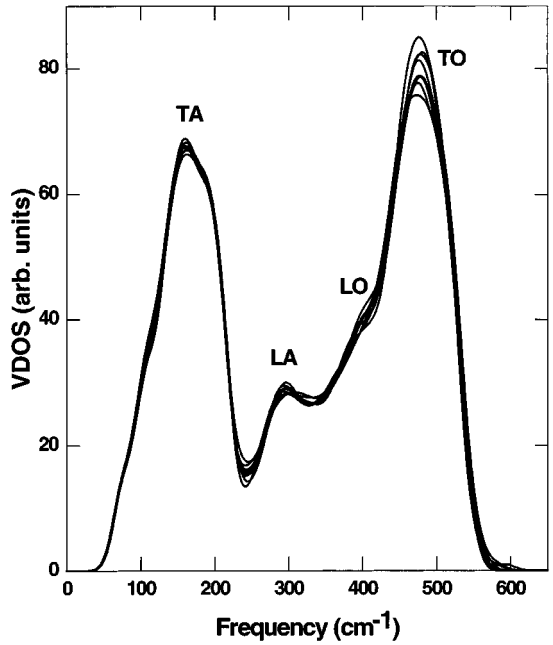

Figure 1. Vibrational density of states (VDOS) of the investigated a-Si models.

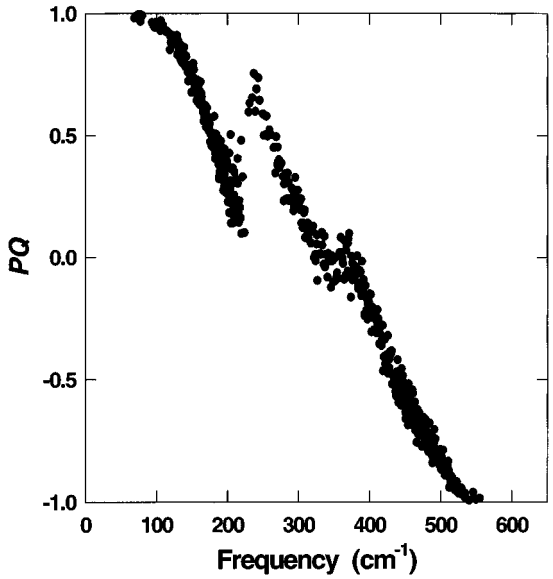

Figure 2. Calculated phase quotient for model 8.

Only the phase quotient for model 8, which has the smallest total energy, is shown in figure 2, because the data for the different models are very similar. Three branches can be clearly distinguished: an acoustic branch in the frequency range 0–200 cm^{-1}; an acoustic branch in the frequency range 250–350 cm^{-1} and an optic branch in the frequency range 400–600 cm^{-1}. The

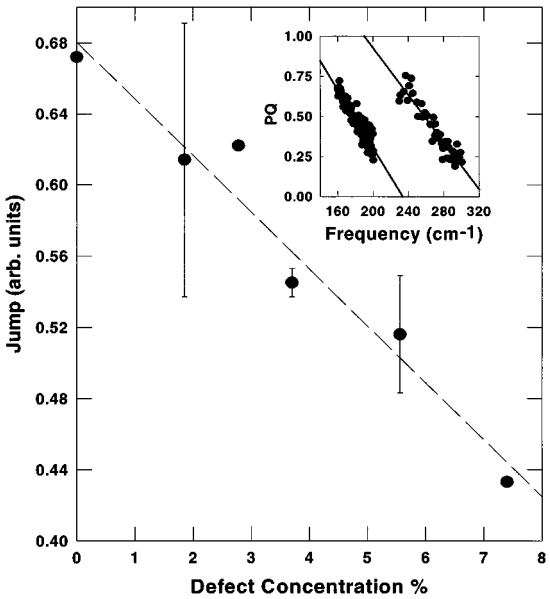

Figure 3. Dependence of the height of the jump in the phase quotient on the total defect concentration. The dashed line is a linear regression fit through the data points with regression coefficient $r = 0.9685$. The inset shows the fit of the low-frequency and the high-frequency branches of PQ for model 8. The dashed lines are linear fits through the data points.

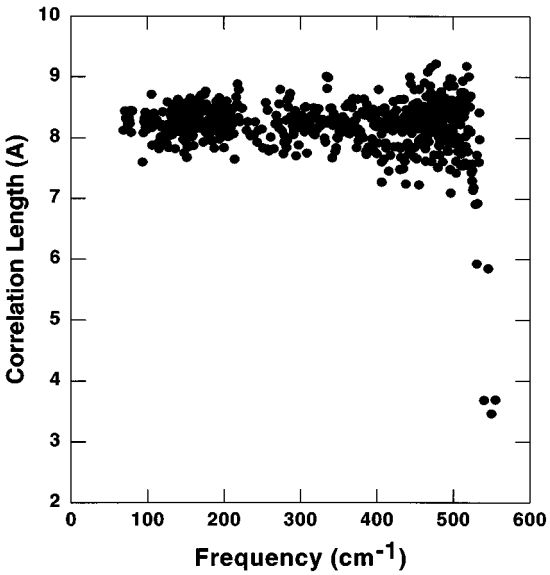

Figure 4. Calculated correlation length as a function of frequency for model 8.

modes above 250 cm^{-1} become increasingly more optic-like with increasing frequency. The major difference between the PQ(ω) data for the different models is in the region of the discontinuity at about 230 cm^{-1}: the height of the jump *decreases* as the total number of coordination defects *goes up* (figure 3). This means that the *mixing* of the TA band at about 160 cm^{-1} with the high-frequency modes increases with increasing defect concentration. The jump values

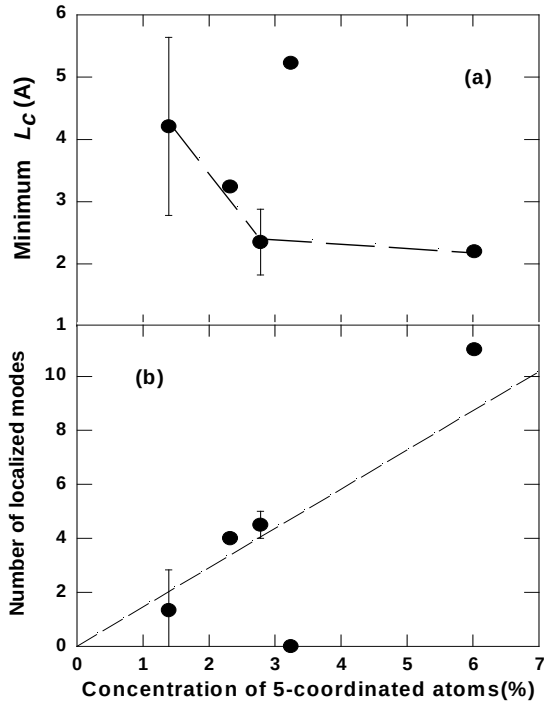

Figure 5. Dependence of the number of strongly localized modes (a) and the minimum correlation length (b) on the concentration of five-coordinated Si atoms. The dashed lines are only a guide for the eye.

h were evaluated by a linear fit through the calculated PQ(ω) points lying within 40 cm^{-1} below and 100 cm^{-1} above the frequency of the jump (see the inset of figure 3). The h values for the models which happened to have the same total number of defects were then averaged. The mean errors are much smaller than the jump value itself. The jump in the phase quotient for the relaxed WWW model of a-Si [31], which has no coordination defects, is in excellent agreement with the trend for the ART models (see figure 3). This indicates that the jump in the phase quotient does not depend on the method of preparation of a-Si models of similar size.

Only the $L_c(\omega)$ data for model 8 are shown in figure 4, because of the great similarity of $L_c(\omega)$ for the different models. The high frequency modes (above 500 cm^{-1}) in all models are strongly localized mainly on D_5 defects and tetrahedra with angular distortions which are two to three times larger than the average angular distortions $\langle\Delta\Theta\rangle$ given in table 1. High-frequency localization due to the presence of fivefold coordinated sites was reported previously by Biswas *et al* [4]. We observe also a few low-frequency modes in the range 90–120 cm^{-1} which are localized on three-coordinated atoms, similarly to Biswas *et al* [4, 7], but the participation ratio and the correlation length of these modes, contrary to the results of Biswas *et al* [4], are much higher than that of the high-frequency modes. Below 500 cm^{-1} all modes are extended.

In order to analyse quantitatively the relationship between defect concentration and high-frequency localization we have plotted the observed minimum correlation length (L_c^{min}) versus the concentration of five-coordinated Si atoms. L_c^{min} decreases non-linearly with increasing D_5 concentration (figure 5(a)) except the data for model 2. In contrast, the number of strongly localized modes (modes with $L_c < 5$ Å) increases almost linearly with increasing D_5 concentration

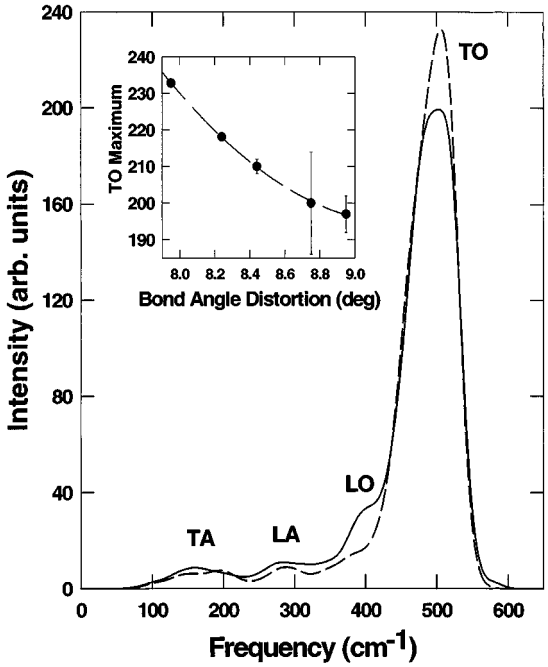

Figure 6. Calculated VV polarized Raman spectra of the models 3 (——) and 8 (- - - -). The inset shows the dependence of the height of the TO Raman peak on the average bond angle distortions $\langle\Delta\Theta\rangle$. The dashed line in the inset is only a guide for the eye.

(figure 5(b)). Accordingly, L_c^{min} for model 7, which has no five-coordinated atoms, is 4.8 Å.

The calculated VV and VH polarized Raman spectra of all models are very similar. That is why only the VV spectra of models 3 and 8 are given in figure 6 for clarity. The average depolarization ratio for all models is 0.57 ± 0.2 in close agreement with experimentally measured depolarization ratios of about 0.5 [11, 23]. The major difference is in the shape and the height of the TO Raman peak. The height of the TO Raman peak decreases with increasing Si–Si–Si bond angle distortions $\langle\Delta\Theta\rangle$ (see the inset of figure 6), which in turn is weakly positively correlated with the total strain energy and the defect concentration of the models. The linewidth of the TO Raman peak in the depolarized (VH) Raman spectra (Γ_{TO}) varies from 74 to 93 cm^{-1}, which compares very well with experimental Γ_{TO} values for a-Si samples prepared by different methods (see for example [10] and [11]). A linear fit of Γ_{TO} as a function of the average bond-angle distortions $\langle\Delta\Theta\rangle$, given in table 1, yields a regression $\Gamma_{TO} = 19.4 \pm 23.7 + 7.1 \pm 2.8\langle\Delta\Theta\rangle$, which within errors is in reasonable agreement with the equation $\Gamma_{TO} = 15 + 6\langle\Delta\Theta\rangle$, proposed by Beeman *et al* [1]. A linear correlation between the frequency of the depolarized TO Raman peak ω_{TO} and Γ_{TO}, $\omega_{TO} = 514.5 \pm 1.1 - 2.7 \pm 0.2\Gamma_{TO}^2/1000$, similar to that proposed by Tsu *et al* [10], is also established. The strain *free* frequency of the TO peak (514.5 ± 1.1 cm^{-1}) is higher than the value of Tsu *et al* [10] probably due to slightly larger choice of homogeneous broadening and stretching force constant. Finally, the TA/TO intensity ratio (I_{TA}/I_{TO}) of the models varies from 0.03 to 0.04, values which are comparable to experimentally measured I_{TA}/I_{TO} ratios for a-Si samples with similar Γ_{TO} [11].

Comparing VDOS and the Raman spectra, it is evident that the TO Raman peak is more sensitive to local tetrahedral distortions than the TO peak in VDOS. We can also see some differences between the spectra in the frequency range 350–430 cm^{-1} (LO peak).

4. Discussion

The results for the jump in PQ(ω), the number of strongly localized modes and their correlation lengths as a function of the defect concentration quantitatively demonstrate that the character of the vibrational modes of a-Si depends on the concentration of coordination defects and tetrahedra with large local strains. Previous calculations of the partial VDOS of four-coordinated Si atoms, using the recursion method [5], also show that increasing the number of five-coordinated nearest neighbours around a regular tetrahedron, i.e. increasing the size of the D_5 defect clusters, depresses the height of the TO peak in the partial VDOS.

Analysis of the calculated total depolarized Raman spectra shows, however, that there is no *direct* correlation between the linewidth Γ_{TO} and the position ω_{TO} of the TO Raman band and the concentration of coordination defects. This could be understood taking into account that internal strains induced by defects can easily propagate through the network by slight readjustment of the neighbouring atoms.

Therefore, in order to study the effect of the coordination defects on the Raman spectra we have calculated the partial Raman spectra (PRSs) of D_3 and D_5 defects (figure 7). The PRSs of the D_3 defects indicate that they contribute mainly to the *low*-frequency part (300–400 cm^{-1}) of the LO band. In contrast the partial Raman spectra of the D_5 defects show that they contribute strongly to the *high*-frequency part (380–460 cm^{-1}) of the LO peak and to the LA Raman peak (300 cm^{-1}). In addition the D_5 defects give rise to a strongly localized peak at about 600 cm^{-1} on the high-frequency side of the TO Raman peak (see the inset of figure 7). The depolarization ratio of the 600 cm^{-1} feature is very low and consequently the high-frequency vibrations of the D_5 atoms represent predominantly symmetric stretching (i.e. breathing) modes.

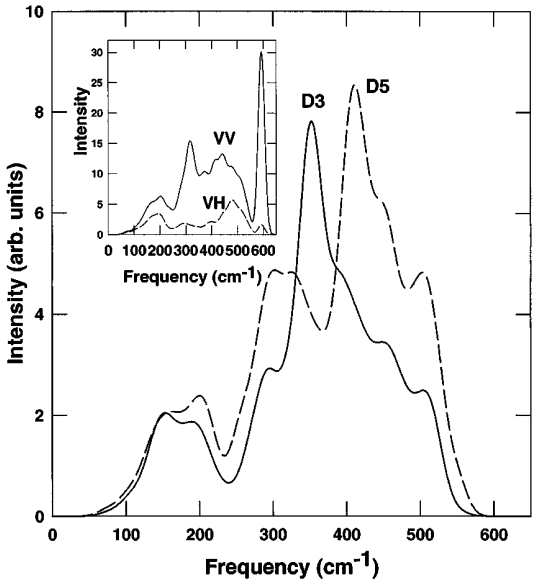

Figure 7. Calculated partial VV polarized Raman spectra of three-coordinated (——) and five-coordinated (– – –) Si atoms in model 8, which happened to have the same number of three- and five-coordinated defects. The inset shows the VV and VH partial Raman spectra of the five-coordinated atoms in model 4 which happens to have two clusters of five-coordinated atoms.

Since the formation of small rings is enhanced by the presence of coordination defects we have calculated also the partial Raman spectra of three- and four-membered rings. The

three-membered rings in models 3 and 6 are formed exclusively by five-coordinated Si atoms and their partial Raman spectra are similar to those of the D_5 defects. The average partial Raman spectra of the four-membered rings in models 3 and 6, which happened to have 14 and six four-membered rings, are shown in figure 8. These spectra clearly show that the peak at about 400 cm^{-1} (LO peak) and the shoulder at about 460 cm^{-1} in the total Raman spectra are enhanced by the presence of four-membered rings. Indeed, the LO peak is of highest intensity for model 3 and is completely missing in the total Raman spectra of model 8 (see figure 6), which happen to have the largest number and zero four-membered rings, respectively. The shoulder at 400 cm^{-1} is also totally absent in the calculated Raman spectra (figure 7 in [14]) of the WWW model which does not have any four-membered rings either [31]. The above-mentioned peak is of a high depolarization ratio and consequently is due to antisymmetric bond stretching vibrations of the four-membered rings.

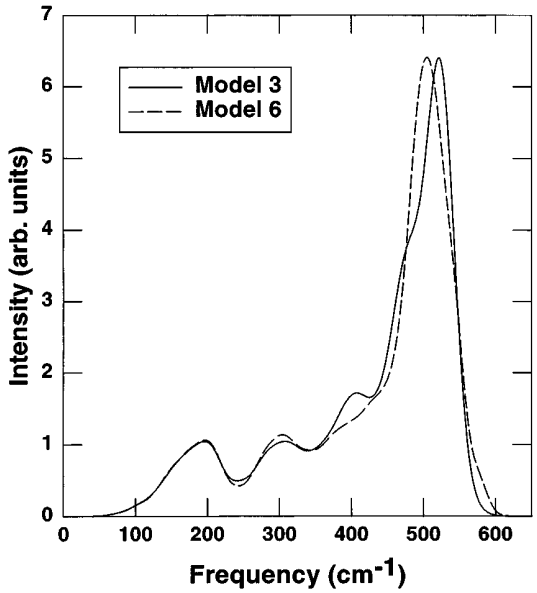

Figure 8. Calculated partial VV polarized Raman spectra of four-membered rings in model 3 (——) and model 6 (- - - -).

The calculated partial Raman spectra suggest that the enhancement of the intensity of the LA and LO Raman peaks of pure and hydrogenated amorphous silicon samples, prepared by radio frequency sputtering (RFS), compared to the spectra of samples prepared by glow discharge (GD) or by chemical vapour deposition (CVD) (see for example [32] and [33]), is probably due to an increase of the concentration of coordination defects and four-membered rings. This interpretation is in agreement with the general conclusion of these authors that the RFS samples have lower network order.

5. Conclusions

The vibrational spectra of amorphous Si models with coordination defects generated by the activation–relaxation technique (ART) are studied by numerical calculations. ART was used because models constructed by WWW-type methods contain intrinsically no coordination defects. The investigated models have similar pair correlation functions and Si–Si–Si bond

angle distributions but different ring distributions and defect concentrations (with up to 8% defects). The latter correlate weakly with the total strain energy and the average bond-angle distortions.

The main features of the polarized Raman spectra are not sensitive to the distribution of large n-membered rings ($n \geqslant 5$) because all atoms in the network participate at least in several five- or six-membered rings. In contrast, they are strongly affected by the short-range order (defect) atomic arrangements: (i) There is a general trend for decreasing the height and increasing the width of the TO and LA peaks in VDOS with increasing defect concentration. (ii) The height of the jump in the phase quotient decreases when the number of coordination defects increases. Therefore, we predict that the separation of the TA and the LA Raman peaks should decrease with increasing defect concentration. (iii) By contrast, the number of modes with short correlation length goes up with the number of coordination defects, due to the increase in the localization of the modes on defects. (iv) The TO Raman peak is not sensitive to the concentration of coordination defects itself but to the *induced* average local strain commonly expressed as the average bond-angle disorder $\langle \Delta\Theta \rangle$. (v) The three- and five-coordinated atoms contribute respectively to the low- and high-frequency parts of the LO Raman peak. (vi) The Raman intensity of the LO peak increases as the number of four-membered rings goes up.

Correspondingly, we predict that the LA–LO region of the Raman spectra is a fingerprint for the presence of three- and five-coordinated Si atoms as well as four-membered rings while the presence of enhanced intensity above 560 cm^{-1} with low depolarization ratio may indicate the presence of clusters of five-coordinated Si atoms in real a-Si materials. An increase of the concentration defects would moreover increase the asymmetry of the TO Raman peak on the low-frequency side. Further detailed studies of the Raman spectra of a-Si samples with different concentration of coordination defects, prepared under identical conditions, would be necessary to test these predictions.

References

[1] Beeman D, Tsu R and Thorpe M F 1985 *Phys. Rev.* B **32** 874
[2] Mousseau N and Lewis L J 1991 *Phys. Rev.* B **43** 9810
[3] Singh J 1981 *Phys. Rev.* B **23** 4156
Tanaka K and Tsu R 1981 *Phys. Rev.* B **24** 2038
Berntsen A J M, van der Weg W F, Stolk P A and Saris F W 1993 *Phys. Rev.* B **48** 14 656
[4] Biswas R, Bouchard A M, Kamitakahara W A, Grest G S and Soukoulis C M 1988 *Phys. Rev. Lett.* **60** 2280
[5] Ishibashi K, Tsumuraya K and Nakata S 1994 *J. Chem. Phys.* **101** 1412
[6] Luchnikov V A, Medvedev N N, Appelhagen A and Geiger A 1996 *Mol. Phys.* **88** 1337
[7] Feldman J L, Allen P B and Bickham S R 1999 *Phys. Rev.* B **59** 3551
[8] Biswas R, Kwon I, Bouchard A M, Soukoulis C M and Grest G S 1989 *Phys. Rev.* B **39** 5101
[9] Chehaidar A, Rouhani M D and Zwick A 1995 *J. Non-Cryst. Solids* **192/193** 238
[10] Tsu R, Hernandez J G and Pollak F H 1984 *J. Non-Cryst. Solids* **66** 109
[11] Maley N, Beeman D and Lannin J S 1988 *Phys. Rev.* B **38** 10 611
[12] Barkema G T and Mousseau N 1996 *Phys. Rev. Lett.* **77** 4358
Mousseau N and Barkema G T 1998 *Phys. Rev.* E **57** 2419
[13] Barkema G T and Mousseau N 1998 *Phys. Rev. Lett.* **81** 1865
[14] Marinov M and Zotov N 1997 *Phys. Rev.* B **55** 2938
[15] Stillinger F H and Weber T A 1985 *Phys. Rev.* B **31** 5262
[16] Mousseau N and Lewis L J 1997 *Phys. Rev. Lett.* **78** 1484
[17] Kirkwood J G 1939 *J. Chem. Phys.* **7** 506
[18] Fortner J and Lannin J S 1989 *Phys. Rev.* B **39** 5527
[19] Bell R J and Hibbins-Butler D C 1975 *J. Phys. C: Solid State Phys.* **8** 787
[20] Alben R, Weaire D, Smith J E Jr and Brodsky M H 1975 *Phys. Rev.* B **11** 2271
[21] Bell R J and Hibbins-Butler D C 1976 *J. Phys. C: Solid State Phys.* **9** 2955

[22] Zotov N, Michailova B, Marinov M and Konstantinov L 1993 *Physica* A **201** 4102
[23] Smith J E Jr, Brodsky M H, Crowder B L and Nathan M I 1971 *Phys. Rev. Lett.* **26** 642
Bermejo D and Cardona M 1979 *J. Non-Cryst. Solids* **32** 405
[24] Mercer J M Jr and Chou M Y 1991 *Phys. Rev.* B **43** 6768
Servalli G and Colombo L 1993 *Europhys. Lett.* **22** 107
Kim E and Lee Y H 1994 *Phys. Rev.* B **49** 1743
[25] Car R and Pirrinello M 1988 *Phys. Rev. Lett.* **60** 204
Fedders P A, Drabold D A, Sankey O E and Dow J D 1990 *Phys. Rev.* B **42** 5135
Clark S J, Crain J and Ackland G J 1997 *Phys. Rev.* B **55** 14 059
[26] Biswas R, Grest G S and Soukoulis C M 1987 *Phys. Rev.* B **36** 7437
[27] Laaziri K, Kycia S, Roorda S, Chicoine M, Robertson J L, Wang J and Moss S C 1999 *Phys. Rev. Lett.* **82** 3460
[28] Kamitakahara W A, Shanks H R, McClelland F, Buchenau U, Gompf F and Pintschovius L 1984 *Phys. Rev. Lett.* **52** 644
[29] Kamitakahara W A, Soukoulis C M, Snaks H R, Buchenau U and Grest G S 1987 *Phys. Rev.* B **36** 6539
[30] Winer K 1987 *Phys. Rev.* **35** 2366
[31] Wooten F, Winer K and Weaire D 1985 *Phys. Rev. Lett.* **54** 1392
[32] Kshirsagar S T and Lannin J S 1982 *Phys. Rev.* B **25** 2916
[33] Morrel G, Katiyar R S, Weisz S Z, Jia H, Shinar J and Balberg I 1995 *J. Appl. Phys.* **78** 5120